JACS
JOURNAL OF THE AMERICAN CHEMICAL SOCIETY
pubs.acs.org/JACS
Article

Reactions of Sodium Diisopropylamide: Liquid-Phase and Solid–Liquid Phase-Transfer Catalysis by *N,N,N′,N″,N″*-Pentamethyldiethylenetriamine

Yun Ma, Ryan A. Woltornist, Russell F. Algera, and David B. Collum*

Cite This: *J. Am. Chem. Soc.* 2021, 143, 13370–13381
Read Online
ACCESS | Metrics & More | Article Recommendations | Supporting Information

ABSTRACT: Sodium diisopropylamide (NaDA) in *N,N*-dimethylethylamine (DMEA) and DMEA–hydrocarbon mixtures with added *N,N,N′,N″,N″*-pentamethyldiethylenetriamine (PMDTA) reacts with alkyl halides, epoxides, hydrazones, arenes, alkenes, and allyl ethers. Comparisons of PMDTA with *N,N,N′,N′*-tetramethylethylenediamine (TMEDA) accompanied by detailed rate and computational studies reveal the importance of the trifunctionality and κ^2–κ^3 hemilability. Rate studies show exclusively monomer-based reactions of 2-bromooctane, cyclooctene oxide, and dimethylresorcinol. Catalysis with 10 mol % PMDTA shows up to >30-fold accelerations (k_{cat} > 300) with no evidence of inhibition over 10 turnovers. Solid–liquid phase-transfer catalysis (SLPTC) is explored as a means to optimize the catalysis as well as explore the merits of heterogeneous reaction conditions.

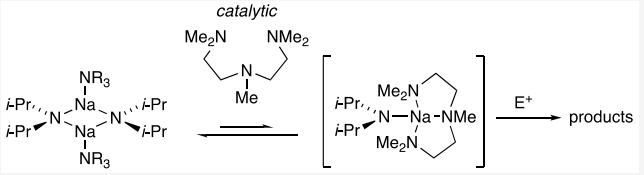

INTRODUCTION

Despite occasional bursts of activity through the last century,[1−6] organosodium chemistry has not kept abreast with organolithium chemistry by any measure.[6,7] The most reactive reagents such as sodium diisopropylamide (NaDA) and *n*-butylsodium that would logically be cornerstones of the discipline suffer from low solubility in inert hydrocarbon solvents and instability in ethereal solvents if not handled correctly.[8] These were solvable problems, and serious progress toward developing convenient, highly reactive bases has been made.[4,5,8−13] Given the lackluster interest from synthetic chemists, it follows that organosodium chemistry has received even less attention from those who care about structure and mechanism. Representation of organosodiums in the crystallographic literature is adequate,[14] but spectroscopic,[15] mechanistic,[16] and even computational studies are sparse.[17]

Our efforts to foster new applications of organosodium chemistry have relied on understanding structure–reactivity principles of NaDA.[12] In this paper, we describe a search for a robust ligand that can *catalyze* NaDA-mediated metalations (eq 1), a plan that brought several seemingly disparate issues into focus.

$$\text{substrate} \xrightarrow[\text{catalytic ligand}]{i\text{-Pr}_2\text{NNa}} \text{product} \qquad (1)$$

Robust Solvents. There is little reason to believe that solvents (ligands) optimized for organolithium chemistry should be optimal for organosodium chemistry as well. Much like other practitioners of organoalkali metal chemistry, however, we have not resisted the siren call to use THF; *all* of our rate and mechanistic studies to date have used THF/hexane mixtures.[7,12] We did this to maximize comparisons with the wealth of data accrued on LDA in THF.[18] THF is an adequate solvent for NaDA, but the half-life to base-mediated destruction ($t_{1/2}$ = 1.0 h at 25 °C)[12b,19] restricts its use for recalcitrant metalations that could most benefit from NaDA's high reactivity.[7,12] NaDA solvated by *N,N,N′,N′*-tetramethylethylenediamine (TMEDA) shown crystallographically to be dimer **4** by Andrews and co-workers[5b] represented an important milestone toward rendering NaDA more convenient, but it remained unnoticed by the synthetic organic chemistry community. NaDA can also be prepared as 1.0 M stock solutions that are stable for months with refrigeration using simple trialkylamines such as *N,N*-dimethylethylamine (DMEA), *N,N*-diethylmethylamine (DEMA), *N,N*-dimethylbutylamine, and *N*-methylpyrrolidine.[7,12b,20] Moreover, these weakly coordinating trialkylamines are substitutionally labile to standard ethereal ligands such as THF.[12b,21]

Crystallographically focused groups such as those of Mulvey and Andrews long ago noticed the merits of polyamines such as *N,N,N′,N′,N″*-pentamethyldiethylenetriamine (PMDTA).[6b,22] We suspected that such polyamines would also elicit high reactivities with highly manageable (limited) decomposition.[12b,19,23] We had examined the structures of a number of NaDA solvates.[12b] Studies of reactivity described in

Received: June 23, 2021
Published: August 10, 2021

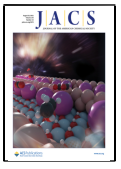

https://doi.org/10.1021/jacs.1c06528
J. Am. Chem. Soc. 2021, 143, 13370–13381

this paper are founded on solution structural studies of amine-solvated dimers **1**−**5**.

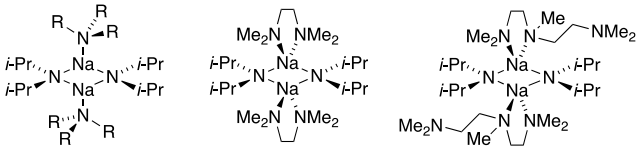

1; R_3N = $EtNMe_2$
2; R_3N = Et_2NMe
3; R_3N = Et_3N

4 **5**

Hemilability. In a 1992 review, we challenged a number of misconceptions about the chelate effect in general and TMEDA in particular.[24] For example, despite TMEDA's reputation for eliciting marked accelerations in organolithium chemistry owing to its putative prowess as a chelating ligand—a prowess we claimed was overstated and poorly understood—stabilization of a rate-limiting transition structure by chelation will be partially, if not entirely, offset by chelation in the reactant (**6**, eq 2). By contrast, if the reactant is *not* chelated (see **7**), then the full advantages of chelation exclusively in the transition state should maximize the putative benefits of the chelate effect.[25] This little-used variant of "hemilability"—most users focus on labile chelates—elicited up to 10^4-fold accelerations for LDA-mediated metalations.[26,27] Could the larger sodium ion support an analogous κ^2−κ^3 hemilabile relationship (eq 3) using PMDTA-solvated dimer **5**?

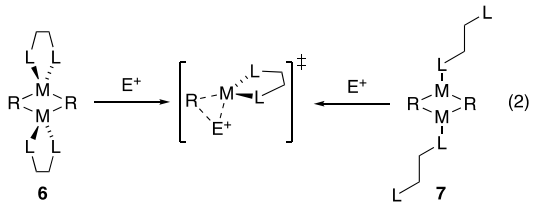

6 **7** (2)

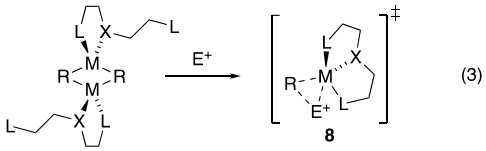

8 (3)

Ligand-Based Catalysis. Imagine the idealized ligand displaying the generality of BINAP [(2,2′-bis-(diphenylphosphino)-1,1′-binaphthyl)] that could be used *catalytically* to modify a wide range of inherently stoichiometric organolithium reactions. It would be transformational. Unfortunately, there are few examples of such ligand-based catalysis in organolithium chemistry.[28−30] We suspect that the high affinities of polydentate ligands for soluble and relatively unhindered lithium salt products such as LiCl (eq 4) sequester ligand and preclude turnovers. Notably, a large proportion of the examples involve additions to imines to form lithium dialkylamides, which, by virtue of their high steric demands, release the ligands.[28−30] We surmised that the *insolubility of inorganic sodium salts* such as NaCl or NaBr would foster turnover (eq 5) and further held an altogether unsupported hope that the sodium ion might release the ligand even from *soluble* sodium salts.

$$\mathrm{R{-}Li + E{-}X \xrightarrow{ligand} R{-}E + (ligand)LiX} \quad (4)$$

$$\mathrm{R{-}Na + E{-}X \xrightarrow{ligand} R{-}E + NaX_{solid} + ligand} \quad (5)$$

Solid−Liquid Phase-Transfer Catalysis (SLPTC). If one can solve the aforementioned problems and achieve acceleration *and* catalysis, any stereo- or regiocontrol necessarily relies on the suppression of the uncatalyzed background reaction. This could be acutely challenging for reactive organosodium-based reagents. We have accrued ample evidence that NaDA in simple trialkylamines displays muted basal reactivities at least relative to THF. A complementary approach, however, would be to exploit a two-phase system in which NaDA is an insoluble solid suspended in a hydrocarbon (eq 6). The catalytically active ligand assumes the role of phase-transfer catalyst and, ideally, isolates the reaction to the solution phase containing only ligated reagent.

$$\mathrm{R{-}Na_{solid} + E{-}X \xrightarrow{ligand\ catalysis} R{-}E + NaX_{solid}} \quad (6)$$

Whereas liquid−liquid phase-transfer catalysis (LLPTC) enjoys considerable notoriety,[31] solid−liquid phase-transfer catalysis (SLPTC) is a much smaller niche.[31b,32,33] Examples of SLPTC are largely proof-of-principle or commodity chemical applications on simple systems.[32] Binaphthyl-based phosphate-catalyzed reactions reported by Toste and co-workers are emblematic of a few standout exceptions.[34−36] Like any heterogeneous reaction, however, complexity can rear its ugly head. Substrates with standard functionalities can solubilize the reagent or cause a reaction to occur on the solid surface at the so-called "omega phase".[32] Further challenges stemming from the heterogeneity include complex reaction orders, occlusion of the insoluble reagent by precipitation of the product,[37] and dependencies on particle size, stir rates, and ultrasound agitation.[36a,38,39] Complexities aside, the importance of understanding the molecular and mechanistic principles underlying SLPTC is enormous given that *any* heterogeneous reaction is implicitly subject to the vicissitudes of SLPTC, and slurries are commonplace inside pharmaceutical process laboratories and production facilities.[40] Why leave studies of these systems to the chemical engineers?

In this paper, we examine the reactivity of NaDA focusing on PMDTA.[6a,22] Both TMEDA and PMDTA facilitate metalations, but PMDTA is far superior, eliciting up to >10^2-fold accelerations attributable to hemilability. Catalysis is optimal when NaBr or NaCl precipitate, but turnover is observed even for reactions affording soluble sodium salts. SLPTC is explored as a means to amplify the *relative* importance of catalysis by suppressing the basal rates. The protocols described herein provide a foundation—the previously derided proof-of-principle experiment—for catalysis that may find concrete applications.

RESULTS AND DISCUSSION

Core observations are summarized in Table 1. Although NaDA can be prepared as a 1.0 M solution in DMEA in a few minutes,[12] we take the added precaution of using NaDA isolated as a white solid because of our emphasis on rate studies. Han and co-workers have provided a direct preparation of NaDA/PMDTA in situ.[13] Reaction rates for the metalations depicted generically in eq 7 were monitored by in situ IR[41] or ^{1}H NMR spectroscopies or by gas chromatographic analyses of quenched samples. Because of product volatilities, the yields are determined relative to internal standards unless explicitly stated otherwise. The relative rate constants (k_{rel}) for homogeneous reactions are measured at constant NaDA and substrate concentration (0.12 M each)

https://doi.org/10.1021/jacs.1c06528
J. Am. Chem. Soc. 2021, 143, 13370−13381

Table 1. PMDTA-Dependent Relative Rate Constants (eq 8) for NaDA-Mediated Metalations (eq 7)

entry	substrate	product	temperature (°C)	yield	k_{PMDTA}
1	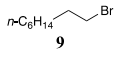 **9**	 **10**	–30	82%	300
2	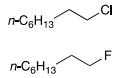	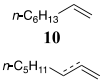 **10**	0	86%	220
3	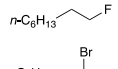	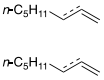	25	—	>200
4	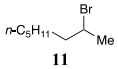 **11**	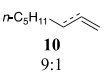 **10** 9:1	0	90%	340
5	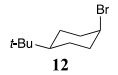 **12**		–30	95%	150
6	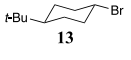 **13**		25	86%	230
7			–80	95%	350
8			0	93%	330
9	 **15**	 **16** (5:1 Z:E)	25	84%	35
10			25	90%	40
11	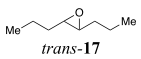 *trans*-**17**	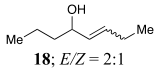 **18**; *E*/*Z* = 2:1	25	89%	70
12	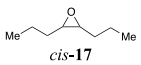 *cis*-**17**	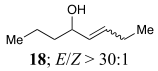 **18**; *E*/*Z* > 30:1	25	91%	20
13	 **19**	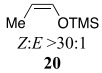 *Z*:*E* >30:1 **20**	0	—	20
14		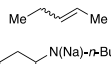	25	85%	85
15		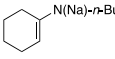	–78	—	45
16		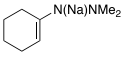	–78	—	35
17	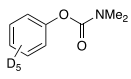	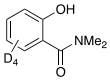	–78	92%	<1
18			–78	—	15

with 10 mol % PMDTA. Catalysis was confirmed when following reactions using 10 mol % PMDTA to full conversion showed neither loss in efficacy nor significant deviation from upwardly curving decays (*vide infra*). The reported values of k_{PMDTA} are gleaned from initial rates referenced to the basal (uncatalyzed) rates according to eq 8. The divisor of 10 in eq 8 accounts for the 10 mol % of catalyst. The basal rates using the less hindered *N*,*N*-diethylmethylamine (DEMA) as the solvent typically fall in the range of 2-fold slower to 3-fold faster than for DMEA,[42] suggesting that DEMA could be used to amplify the relative impact of catalysis in select cases.

Accelerations using 100 mol % (>1.0 equiv) PMDTA are 3–6-fold (rather than 10-fold) higher when compared with 10% PMDTA owing to concentration dependencies delineated below. Moreover, rather than cluttering Table 1 with additional comparisons, we simply note that metalations using 1.0 equiv of PMDTA proceed at rates comparable to analogous reactions in neat THF described previously.[12,43] Large differences between TMEDA and PMDTA confirm the importance of hemilability.

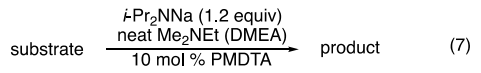

(7)

$$k_{rel} = (k_{DMEA} + k_{PMDTA}/10)/k_{DMEA} \quad (8)$$

Although many of the reactions in Table 1 are self-explanatory, some require additional comment. The elimination of 1-fluorooctane (entry 3) fails in THF owing to THF decomposition, illustrating the advantages of a robust ligand.[12e] The accompanying isomerization of the resulting terminal alkene studied previously for NaDA/THF,[12c] however, is unavoidable under the forcing conditions. The 9:1 regioselectivity for the elimination of 2-bromooctane to form 1-octene (entry 4) is lower than the >30:1 selectivity observed in THF,[12e] which is the highest reported to date for such a base-mediated elimination of **11**.[44] The relative rates for axial and equatorial eliminations (entries 5 and 6) are surprisingly similar ($k_{ax}/k_{eq} \approx 10$ adjusted for the temperature differential). This was also observed for NaDA/THF and traced to E2-like axial elimination of **12** and carbene-based equatorial elimination of **13**.[12e]

The contrasting stereocontrol in *cis* and *trans* epoxides in entries 11 and 12 is precedented for other bases.[45,46] Only a few base-mediated eliminations of the *trans* isomer in entry 11 are reported,[46] presumably stemming, in part, from an aversion to reporting poor selectivities. Terminal epoxides (not shown) lead to oligomerization to form polyethers. Entries 16–18 reveal little acceleration by PMDTA, which could arise from high basal reactivities of the uncatalyzed reaction or because the tridentate ligand suppresses requisite substrate coordination to sodium at the transition state. The metalation in eq 9 illustrates a regioselectivity that had been studied using NaDA/THF.[12e] We thought that PMDTA might suppress a facile equilibration with an alternative regioisomer ortho to the chloro, but the selectivity suggests that equilibration intervened.

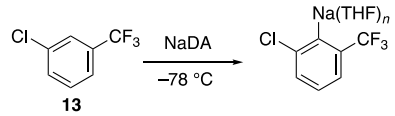

(9)

Some arenes undergo partial orthometalation, displaying soft equilibria with both unmetalated and metalated forms coexisting (eq 10). We hoped that PMDTA might improve such a balanced equilibrium observed with both NaDA/THF[12d] *and* LDA/THF[47] by selectively binding to the aryl sodium, but a soft equilibrium was observed yet again. Rate studies akin to those described below reveal a monomer-based metalation (Supporting Information).

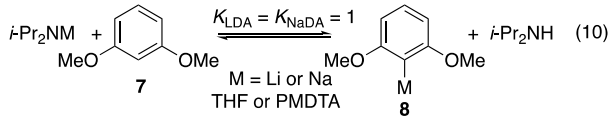

(10)

Acceleration and Catalysis. Acceleration and turnover (catalysis) are described using several cases emblematically.

https://doi.org/10.1021/jacs.1c06528
J. Am. Chem. Soc. 2021, 143, 13370–13381

Dehydrohalogenation of **9** (Table 1, entry 1) with equimolar NaDA in DMEA is slow at −30 °C (Figure 1). After

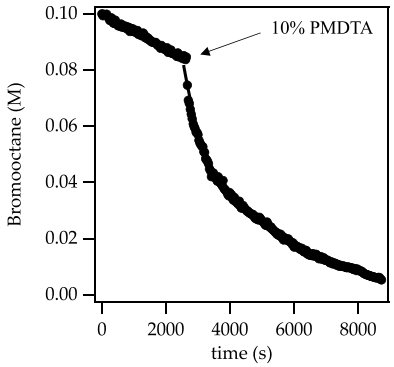

Figure 1. Metalation of 0.10 M **9** with 0.12 M NaDA in neat DMEA at −30 °C monitored by ^{1}H NMR spectroscopy. PMDTA (0.010 M, 0.10 equiv) was injected (see arrow).

establishing a basal rate, 10 mol % (per sodium) PMDTA is injected (see arrow). Precipitation of NaBr is an excellent visual cue that the reaction has commenced. The accelerated metalation proceeds to completion through the requisite 10 turnovers with no noticeable stalling. 1-Octene is formed in 82% ^{1}H NMR yield relative to an internal benzene standard. No N-alkylation (<5%) occurs for the NaDA/THF variant[12c] as evidenced by ^{1}H NMR spectroscopy and GC-MS with comparison to a sample of $(i\text{-Pr})_2NC_8H_{17}$. By contrast, catalytic TMEDA shows no detectable acceleration, which is consistent with recent studies of NaHMDS showing that TMEDA is a mediocre chelating ligand.[48]

Elimination of epoxide **15** (Table 1, entry 10) by 1.2 equiv of NaDA followed by 10 mol % PMDTA shows catalysis with attenuated acceleration (Figure 2). Notably, the product

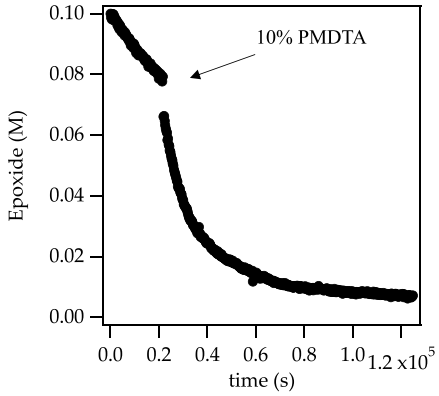

Figure 2. Metalation of 0.010 M cyclooctene oxide (**15**) with 0.12 M NaDA in 1.0 M DMEA at 25 °C monitored by ^{1}H NMR spectroscopy. PMDTA (0.10 equiv, 10 mol %) was injected (arrow).

alkoxide does not precipitate from solution, yet there is no evidence of autoinhibition. If, for example, PMDTA was binding appreciably but reversibly to the alkoxide in a 1:1 stoichiometry, one would expect a burst of reaction to 10% conversion followed by a return to the basal rate. Such biphasic kinetics are not observed. Similarly, autoinhibition owing to the formation of an unreactive i-Pr$_2$NNa−RONa mixed dimer[6a,49] could have caused slowing or stalling at 50% conversion (provided a mixed-aggregate-based metalation does not emerge concurrently); no such inhibition at 50% conversion is observed. The elimination of epoxide **15** plays a central role during investigations of SLPTC (*vide infra*).

We examined tetramines **25** and **26** to ascertain if tetradentate binding might be superior.[50] Muted rates relative to PMDTA suggest that three-coordinate binding is preferred and that the added steric demands are detrimental. Various polyethers were avoided assiduously owing to facile decomposition.[12b]

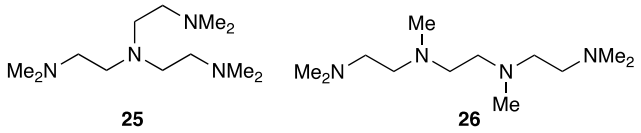

Mechanisms: General. Rate studies were carried out using the method of initial rates[51−53] and monitored using either ^{1}H NMR spectroscopy or GC analysis of quenched aliquots.[54] All transition structures were examined using density functional theory (DFT) computations[55] carried out at the M06-2X level of theory.[56−58] (The computations described herein are archived in the Supporting Information.)

The solvent substitution in eq 11 (A = NaDA subunit; S = DMEA; L = TMEDA or PMDTA) illustrates the structural foundations underlying the rates.[12b] It would be possible but foolhardy to attempt to understand the basic principles of NaDA-mediated metalations under conditions in which the structure of NaDA is shifting from A_2S_2 to A_2LS to A_2L_2. We ring-fenced the complexity by carrying out the bulk of the rate studies at low DMEA concentrations and high TMEDA or PMDTA concentrations, which strongly favor A_2L_2. A high enthalpic preference for A_2L_2 relative to A_2S_2 at reduced temperatures further promotes its formation. Although we avoid conditions favoring A_2LS for the detailed rate studies, A_2LS is mechanistically important under conditions of catalysis (*vide infra*).

$$A_2S_2 + 2L \overset{K_1}{\rightleftharpoons} A_2SL + L + S \overset{K_2}{\rightleftharpoons} A_2L_2 + 2S \quad (11)$$

Mechanism of Cyclooctene Oxide Elimination. Mechanistic principles common to all of the metalations are illustrated with the metalation of cyclooctene oxide (eq 12). A plot of initial rates versus PMDTA concentration (Figure 3) shows that the metalation rate saturates at low DMEA concentrations (curve a) resulting from the full conversion of A_2S_2 to A_2L_2. The observed rate at full saturation is indistinguishable from that observed in the absence of DMEA, conditions in which A_2L_2 is shown spectroscopically to form quantitatively.[12b] In neat DMEA, by contrast, saturation is not achieved (curve b); mixed solvate A_2LS remains dominant. Figure 3 is a reminder of a recurring theme of the probative power of kinetics to study solvation as a molecular phenomenon.

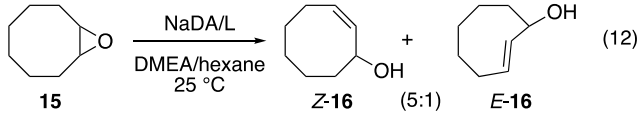

(12)

Under conditions favoring full saturation, metalation of **15** displays a half-order NaDA dependence (Figure 4). The saturation kinetics and the NaDA order are described by the generalized and idealized[59] rate law in eq 13 and mechanism in eqs 15−17. At saturation, the rate law reduces to eq 14 and the mechanism to eqs 16 and 17.

https://doi.org/10.1021/jacs.1c06528
J. Am. Chem. Soc. 2021, 143, 13370−13381

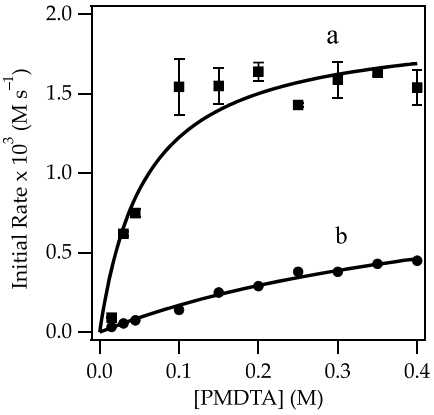

Figure 3. Plot of initial rates versus [PMDTA] in 1.0 M DMEA in hexanes cosolvent for the elimination of cyclooctene oxide (0.067 M) in the presence of 0.10 M NaDA at 25 °C. Curves depict unweighted least-squares fits to $y = ax/(1 + bx)$. Curve a (1.0 M DMEA/toluene): $a = (3.5 \pm 0.9) \times 10^4$; $b = (1.9 \pm 0.6) \times 10^4$. Curve b (neat DMEA): $a = (2.0 \pm 0.2) \times 10^3$; $b = (1.7 \pm 0.4) \times 10^3$.

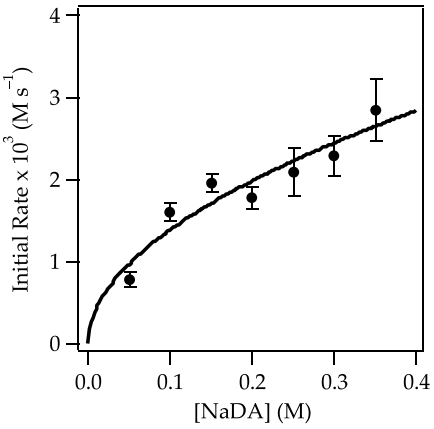

Figure 4. Plot of initial rate versus [NaDA] in 1.0 M DMEA in hexane cosolvent for the elimination of cyclooctene oxide (0.067 M) in the presence of 2.0 M PMDTA at 25 °C. The curve depicts an unweighted least-squares fit to $y = k[\text{NaDA}]^n$: $k = (4.6 \pm 0.7) \times 10^3$; $n = 0.5 \pm 0.1$.

$$-\mathrm{d}[\mathrm{E}^+]/\mathrm{d}t = k[\mathrm{E}^+][\mathrm{A}_{2(\mathrm{total})}]^{1/2}[\mathrm{L}]/(1 + k'[\mathrm{L}]) + c \quad (13)$$

$$-\mathrm{d}[\mathrm{E}^+]/\mathrm{d}t = k[\mathrm{E}^+][\mathrm{A}_2\mathrm{L}_2]^{1/2} \quad (14)$$

$$\underset{(\mathbf{2})}{1/2\mathrm{A}_2\mathrm{S}_2} + \mathrm{L} \overset{K'}{\rightleftharpoons} \underset{(\mathbf{4}\text{ or }\mathbf{5})}{1/2\mathrm{A}_2\mathrm{L}_2} + \mathrm{S} \quad (15)$$

$$\underset{(\mathbf{4}\text{ or }\mathbf{5})}{1/2\mathrm{A}_2\mathrm{L}_2} \overset{K''}{\rightleftharpoons} \underset{(\mathbf{27})}{\mathrm{AL}} \quad (16)$$

$$\underset{(\mathbf{27})}{\mathrm{AL}} + \mathrm{E}^+ \overset{k}{\rightarrow} \underset{(\mathbf{28})}{[\mathrm{ALE}^+]^{\ddagger}} \quad (17)$$

The half-order in NaDA and first-order in substrate suggest that reactions under standard synthetic conditions using equimolar NaDA and substrate ([E] = [A_{total}]) should be 1.5-order overall. As a largely academic exercise, metalation of **15** and several other substrates were fitted to the nonlinear Noyes equation (eq 18)[60] to determine the overall reaction order, *n*, by *best fit*. Although the inherently large error bars have kept the Noyes equation in the shadows,[12b,61] all afforded $1.0 < n < 2.0$.

$$[\mathrm{E}] = ((n - 1)k_{\mathrm{obsd}} + [\mathrm{E}_0]^{-(n-1)})^{-1/n-1} \quad (18)$$

Under conditions of ligand-*catalyzed* metalations (10 mol % PMDTA), the metalations would likely proceed via the same monomer-based transition structure, but the low L concentration with excess A_2S_2 imposes the formation of A_2LS (eq 11), a preference that is enhanced by correlated solvation ($K_1 > K_2$).[12b,62,63] The same monomer-based metalation originating from a different ground state results in quite different concentration dependencies as described by eqs 19−21. The rate law predicts a zeroth-order DMEA dependence and an inverse-half-order dependence on NaDA. (Such a fractional-order *inhibition* by NaDA was observed for 1-pentene isomerization as illustrated in Figure 5.) It suggests that

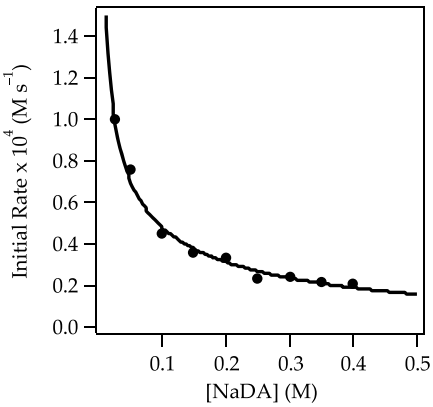

Figure 5. Plot of initial rate versus [NaDA] in DMEA for the isomerization of 1-pentene (0.050 M) in the presence of 10% PMDTA at 25 °C. The curve depicts an unweighted least-squares fit to $y = ax^n + c$ ($a = (2.3 \pm 1.0) \times 105$, $c = (1.9 \pm 0.4)$, $n = (-0.48 \pm 0.11)$.

suppressing the NaDA concentration by slow addition would amplify the *relative* influence of catalysis, k_{rel}, in eq 8. Promotion of catalysis and suppression of the basal rate, k_{DMEA}, by lowering the concentration of A_2S_2 should maximize the influence of catalysis on selectivity.

$$\mathrm{A}_2\mathrm{SL} \overset{K_3}{\rightleftharpoons} 1/2\mathrm{A}_2\mathrm{S}_2 + \mathrm{AL} \quad (19)$$

$$\mathrm{AL} + \mathrm{E}^+ \overset{k'}{\rightarrow} [\mathrm{ALE}^+]^{\ddagger} \quad (20)$$

$$\text{rate} \propto [\mathrm{A}_2\mathrm{LS}]^1[\mathrm{A}_2\mathrm{S}_2]^{-1/2}[\mathrm{S}]^0 \quad (21)$$

Deuterated epoxide **15**-d_2 (eq 22) held promise to demonstrate both the expected kinetic isotope effect on the elimination as well as ruling out carbenoid-based mechanisms. Unfortunately, we observed significant washing out of the deuteriums in the products and recovered epoxide, suggesting a reversible metalation (eq 23). Although it appeared as though the elimination *per se* occurs via a 1,2-elimination, the exchange undermined the experiment, while the source of the protons remained elusive.[64]

https://doi.org/10.1021/jacs.1c06528
J. Am. Chem. Soc. 2021, 143, 13370−13381

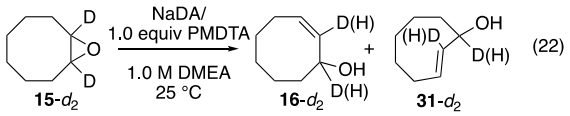

(22)

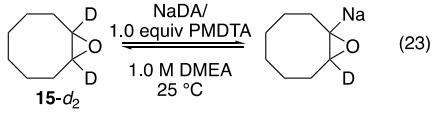

(23)

The accelerations by PMDTA when compared with TMEDA attest to the hemilability (eq 24). The computed transition structure depicted generically as $[ALE^+]^‡$ in eq 17 is shown as **29** in Figure 6.

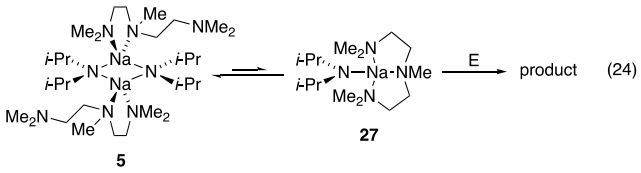

(24)

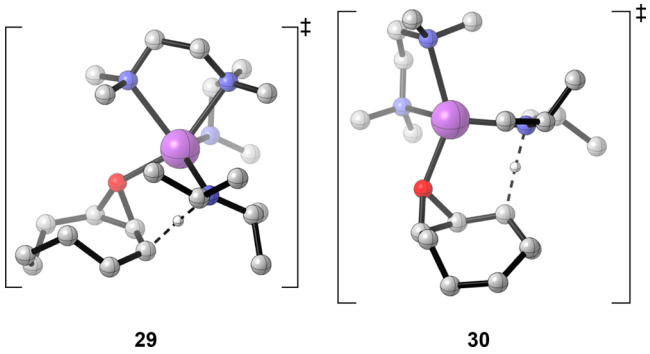

Figure 6. Computed monomer-based transition structures for the elimination of cyclooctene oxide by NaDA/PMDTA (**29**) and NaDA/TMEDA (**30**).

Because of the central importance of TMEDA in organic chemistry, we determined the TMEDA dependence for the elimination of cyclooctene oxide in TMEDA/DMEA and observed saturation kinetics with a 2-fold acceleration off the basal rate (Figure 7). The concentration of TMEDA in which saturation is attained attests to a similar binding constant as PMDTA. Transition structure **30** of stoichiometry $[ALE^+]^‡$ is shown in Figure 6.

Mechanisms of Dehydrohalogenations. Analogous rate studies for the PMDTA-mediated elimination of 1-bromoctane (Table 1, entry 1) afford rate data consistent with eqs 13−17. Monitoring 2,2-d_2-**9** (eq 25) shows an isotopic distribution and isotope effect that confirms a standard vicinal elimination such as the anti elimination via transition structure **31** (Figure 8).[65] The analogous syn elimination via **32** displaying a distinct Na−Br contact was not experimentally excluded but is calculated to be of comparable stability to **31**. Although not studied thoroughly, the isotopically labeled chloro analogue (eq 26) shows an isotope effect and product distribution consistent with a carbenoid mechanism studied previously using NaDA/THF.[12e]

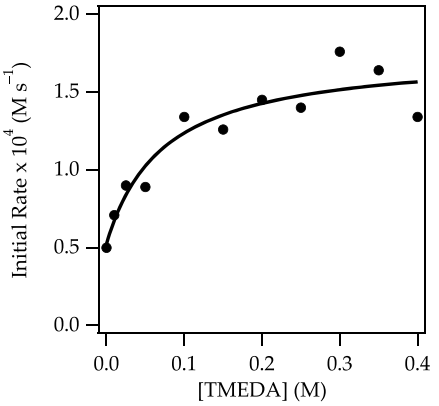

Figure 7. Plot of initial rates versus [TMEDA] in 1.0 M DMEA in hexanes cosolvent for the elimination of cyclooctene oxide (0.067 M) in the presence of 0.10 M NaDA at 25 °C. Curves depict unweighted least-squares fits to $y = ax/(1 + bx) + c$: $a = (1.7 \pm 0.9) \times 10^5$; $b = (1.4 \pm 0.8) \times 10^5$; $c = 0.53$ (set by measurement).

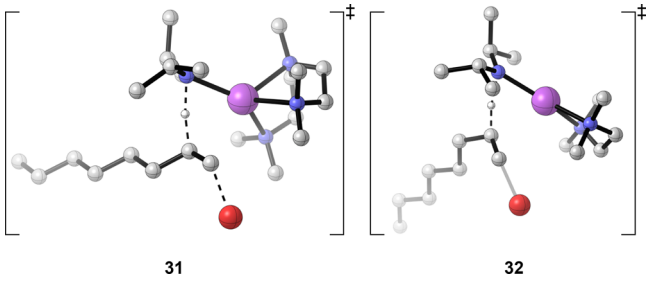

Figure 8. Computed transition structures for the elimination of 1-bromooctane by NaDA/PMDTA (**31**) and NaDA/TMEDA (**32**).

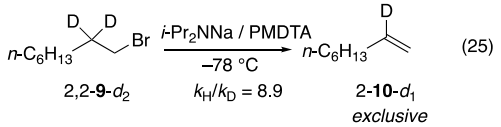

(25)

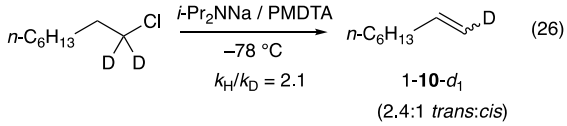

(26)

Solid−Liquid Phase-Transfer Catalysis. Attempts to reduce the basal reactivity using triethylamine afforded marginal solubility, prompting us to consider using suspensions of NaDA in hydrocarbons and employing the polyamines as phase-transfer catalysts. Dehydrobromination of 1-bromooctane (**9**) by a suspension of NaDA at −15 °C revealed a barely measurable basal reaction (Figure 9). Addition of 10 mol % PMDTA elicits a 40-fold acceleration with full conversion attesting to 10 turnovers. The solid-to-solid conversion without stalling shows that occlusion of the NaDA by deposited NaBr is not a problem.[37] Moreover, the upward curvature is consistent with a constant (steady-state) concentration of NaDA−PMDTA[66] superimposed on a first-order dependence of **9**. (Titrations of solid NaDA in hexane with PMDTA or TMEDA formed A_2L_2 (**4** or **5**) linearly proportional to added "L" with no evidence of partial solvate A_2L.)[12b] A plot of initial rates versus PMDTA concentration is akin to a plot versus A_2L_2 concentration and reveals an order on the high side of a half-order (Figure 10). The mechanism is described by eqs 27−29 with transition structure **31** (Figure 8)

https://doi.org/10.1021/jacs.1c06528
J. Am. Chem. Soc. 2021, 143, 13370−13381

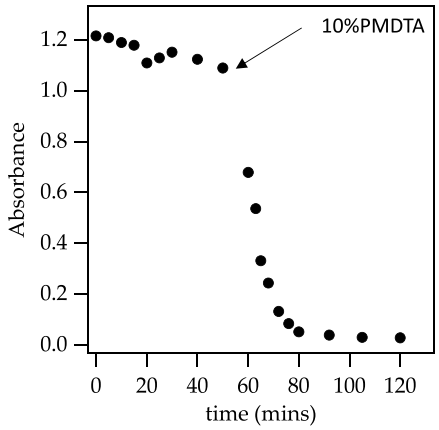

Figure 9. Metalation of 0.15 M **9** with solid NaDA (equiv of 0.16 M) suspended in hexane at −15 °C monitored by GC analysis of quenched aliquots. PMDTA (0.016 M, 0.10 equiv) was injected (see arrow).

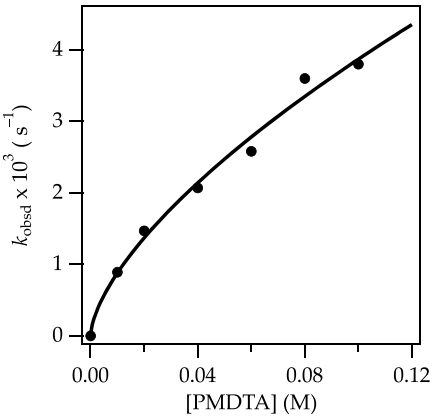

Figure 10. Plot of initial rates versus [PMDTA] in hexanes for the elimination of bromooctane **9** (0.050 M) in the presence of 0.10 M NaDA at −40 °C. The curve depicts an unweighted least-squares fit to $y = ax^n$: $a = (1.7 \pm 0.03) \times 10^2$; $n = 0.65 \pm 0.08$.

shown in the rate studies above. Similar results for SLPTC using TMEDA are observed but with muted accelerations as noted above.

$$-\mathrm{d[E^+]}/\mathrm{d}t = k[\mathrm{E^+}][\mathrm{A_2L_2}]^{1/2} \quad (27)$$

$$\mathrm{A}_{n(\mathrm{solid})} + \mathrm{L} \overset{K_{eq}}{\rightleftharpoons} \underset{(\mathbf{s})}{\mathrm{A_2L_2}} \quad (28)$$

$$1/2\mathrm{A_2L_2} + \mathrm{E^+} \overset{k}{\rightarrow} [\mathrm{ALE^+}]^{\ddagger} \quad (29)$$

SLPTC of epoxide elimination is challenging and underscores a potential limitation of the strategy because epoxides also function as ethereal ligands and can mediate phase transfer, imposing elevated basal rates.[67] Cyclooctene oxide offers a particularly interesting view owing to differential selectivities with and without catalysis (eq 30). In the absence of added ligand, NaDA-mediated metalation of **15** in hexane affords a mixture of *cis* cyclooctenol *Z*-**16**, *trans* cyclooctenol *E*-**16**, and carbene-derived alcohol **39**. Alcohols *Z*-**16** and *E*-**16** are observed in NaDA/DMEA-mediated elimination.[12a] Alcohols *Z*-**16** and **39** are formed in lithium amide-mediated eliminations.[68] Moreover, the reaction becomes homogeneous at approximately 50% conversion. Although, in principle, this could reflect the solubility limit of NaDA solvated by epoxide **15**, we suspect that soluble mixed aggregates are involved.[69]

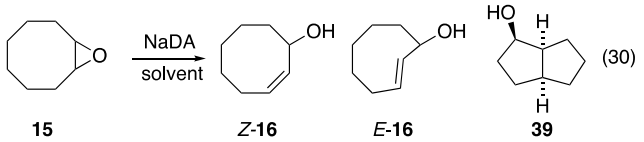

solvent	Z-16:E-16:39
hexane	4:1:6
1.0 equiv PMTDA/hexane	40:8:1
10 mol % PMDTA/hexane	10:2:1

Most importantly, the distribution of *Z*-**16** and (*E*-**16** + **39**) (an unresolved nearly 1:1 mixture) serves as a fingerprint of the polyamine-free elimination, offering an independent measure of the relative contributions of uncatalyzed and catalyzed elimination that complements that derived from ligand-dependent metalation rates. Table 2 illustrates the product distribution measured vs PMDTA concentration.

Table 2. Product Ratios for the Elimination of Cyclooctene Oxide with NaDA in Hexane in the Presence of PMDTA

PMDTA (mol %)	(*Z*-**16**+*E*-**16**):**39**
0	0.7
5	7
10	12
5[a]	14
100	50

[a]Slow addition over 9 h with a syringe pump.

Taken together, minimizing the epoxide concentration should minimize the basal rate *relative to the catalyzed rate*. To test this hypothesis, we dropped the catalyst loading to 5 mol %, which affords a particularly poor selectivity consistent with a high *relative* basal rate (Table 2). Rapid addition affords a 7:1 selectivity consistent with the basal and catalyzed rates near parity. Slow addition by motor-driven syringe over 9 h reveals a measurably improved 14:1 *relative rate* of the catalyzed elimination (Table 2). Thus, using SLPTC to catalyze a reaction in which the substrate can mediate its own metalation will witness significant substrate concentration dependencies. Most substrates have ligating functionality; one could imagine high coordination numbers in the substrate-mediated substrate metalations in organosodium chemistry.

CONCLUSIONS

The work described above covers considerable intellectual territory and is a lot to digest. Those interested in crystallography have certainly noticed the merits of PMDTA as a trifunctional ligand for sodium.[6b,22] Its capacity to serve as a base-resistant, highly efficacious surrogate for THF leads us to suspect that PMDTA may play a central role if organosodium chemistry pushes its way into more mainstream applications.

The importance of hemilability, which relies on elevated coordination numbers in the rate-limiting transition structures relative to the reactants, is also a promising construct. To foreshadow hemilability in other NaDA-mediated reactions, one could start by measuring the efficacies (rates) of PMDTA versus TMEDA. We are reminded once again that rate studies are a particularly powerful means of studying metal ion

https://doi.org/10.1021/jacs.1c06528
J. Am. Chem. Soc. 2021, 143, 13370−13381

solvation by capturing the fleeting solvation events beyond the view of the various spectroscopies.

It would be premature to declare that organosodium chemistry will be catapulted forward by the benefits of ligand-based catalysis in a broad sense, but catalysis of NaDA-mediated metalations is encouraging. Let us consider alkylations of seemingly related sodiated imines or hydrazones (eq 31), which have been alkylated enantioselectively as the lithium salt using stoichiometric sparteine by McClacken and co-workers.[70] It does not take a particularly fertile mind to imagine how chiral PMDTA analogues might impart enantioselectivity and do so catalytically. Of course, there remain significant hurdles to overcome before credible applications of catalyzed organosodium chemistry emerge. We are not well-positioned to do this justice; crowdsourcing this to the free market of ideas where specific needs drive the solutions is more appropriate anyway.

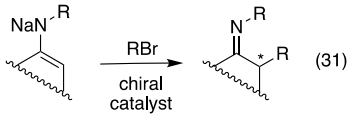

(31)

During efforts to maximize the relative influence of catalyzed metalations, we turned to SLPTC to optimize potentially beneficial stereo-, regio-, or chemoselectivities imparted by catalysis. As above, it is a minor extrapolation to imagine using SLPTC on other hexane-insoluble organosodium or even organolithium reagents. Thinking more generally, we wonder if instead of focusing on catalytically active discrete organo-transition catalysts one might focus on stoichiometric reactions of inexpensive first-row transition metals that could be *catalyzed* by designer ligands. Once again, we leave this thought for others to ponder.

SLPTC is already a very broad topic in that suspensions are commonplace in pharmaceutical process laboratories and plants. The functional molarity of a heterogeneous reaction—the moles per liter within a vat—is constrained by the quantity and physical properties of the insoluble reagent and the size of the paddle. Although the engineers are particularly good at solving such technical problems—they have very big paddles—we wonder if the solid–liquid phase-transfer problems *inherent* to heterogeneous reactions might benefit from additional molecular-level scrutiny.

EXPERIMENTAL SECTION

Reagents and Solvents. PMDTA, TMEDA, DMEA, DEMA, and hexane were distilled from solutions containing sodium benzophenone ketyl. NaDA was prepared as described previously.[12b] Solutions of NaDA can be titrated for active base using a literature method.[71] Air- and moisture-sensitive materials were manipulated under argon using standard glovebox, vacuum line, and syringe techniques.

NMR Spectroscopy. Individual stock solutions of substrates and NaDA were prepared at room temperature. An NMR tube under vacuum was flame-dried on a Schlenk line and allowed to return to room temperature. It was then backfilled with argon and placed in a −78 °C dry ice/acetone bath. The appropriate amounts of NaDA (1.1 equiv) and substrate were added sequentially via syringe. The tube was sealed under partial vacuum, vortexed three times on a vortex mixer for 5 s, and dropped into the precooled spectrometer. Standard ^{1}H and ^{13}C NMR spectra were recorded at 500 and 125.79 MHz, respectively. The ^{1}H and ^{13}C resonances are referenced to Me_4Si (0.0 ppm).

Representative Reaction of 15. To a stirred solution of NaDA (200 mg, 1.62 mmol) in dry hexane (6 mL) containing PMDTA (281 mg, 1.62 mmol) under an argon atmosphere at 25 °C was added epoxide **15** (189 mg, 1.50 mmol) in hexane (4.0 mL). The reaction mixture was stirred for 1.2 h, quenched by the addition of saturated NH_4Cl solution (4 mL), and extracted with ether (3 × 8.0 mL). The organic layer was washed with brine (8 mL) and dried over Na_2SO_4. Evaporation of solvent followed by flash chromatography of the resulting crude residue using hexane/ether (5/1) as eluent afforded an E/Z mixture of *Z*-**16** (138 mg, 73% yield) and *E*-**16** (34 mg, 18% yield) displaying spectroscopic data consistent with literature values.[72]

ASSOCIATED CONTENT

Supporting Information

The Supporting Information is available free of charge at https://pubs.acs.org/doi/10.1021/jacs.1c06528.

Spectral, rate, and computational data (PDF)

AUTHOR INFORMATION

Corresponding Author

David B. Collum − *Department of Chemistry and Chemical Biology, Baker Laboratory, Cornell University, Ithaca, New York 14853−1301, United States;* orcid.org/0000-0001-6065-1655; Email: dbc6@cornell.edu

Authors

Yun Ma − *Department of Chemistry and Chemical Biology, Baker Laboratory, Cornell University, Ithaca, New York 14853−1301, United States*

Ryan A. Woltornist − *Department of Chemistry and Chemical Biology, Baker Laboratory, Cornell University, Ithaca, New York 14853−1301, United States*

Russell F. Algera − *Department of Chemistry and Chemical Biology, Baker Laboratory, Cornell University, Ithaca, New York 14853−1301, United States*

Complete contact information is available at: https://pubs.acs.org/10.1021/jacs.1c06528

Notes

The authors declare no competing financial interest.

ACKNOWLEDGMENTS

We thank the National Institutes of Health (GM131713) for support.

REFERENCES

(1) Schorigin, P. Synthesen mittels Natrium und Halogenalkylen. *Ber. Dtsch. Chem. Ges.* **1908**, *41*, 2711.

(2) (a) Gilman, H.; Wright, G. F. The Mechanism of the Wurtz—Fittig Reaction. The Direct Preparation of an Organosodium (Potassium) Compound from an RX Compound. *J. Am. Chem. Soc.* **1933**, *55*, 2893. (b) Gilman, H.; Breuer, F. Relative Aromaticities. IV. Furyl-Alkali Compounds. *J. Am. Chem. Soc.* **1934**, *56*, 1123.

(3) Morton, A. A. The Chemical Behavior of the Organoalkali Compounds. *Chem. Rev.* **1944**, *35*, 1.

(4) Lochmann, L.; Janata, M. 50 Years of Superbases Made from Organolithium Compounds and Heavier Alkali Metal Alkoxides. *Eur. J. Chem.* **2014**, *12*, 537.

(5) (a) Barr, D.; Dawson, A. J.; Wakefield, B. J. A Simple, High-Yielding Preparation of Sodium Diisopropylamide and Other Sodium Dialkylamides. *J. Chem. Soc., Chem. Commun.* **1992**, 204. (b) Andrews, P. C.; Barnett, N. D. R.; Mulvey, R. E.; Clegg, W.; O'Neil, P. A.; Barr, D.; Cowton, L.; Dawson, A. J.; Wakefield, B. J. X-ray Crystallographic Studies and Comparative Reactivity Studies of a Sodium Diisopropylamide (NDA) Complex and Related Hindered Amides. *J. Organomet. Chem.* **1996**, *518*, 85.

(6) (a) Mulvey, R. E.; Robertson, S. D. Synthetically Important Alkali-Metal Utility Amides: Lithium, Sodium, and Potassium Hexamethyldisilazides, Diisopropylamides, and Tetramethylpiperidides. *Angew. Chem., Int. Ed.* **2013**, *52*, 11470. (b) Robertson, S. D.; Uzelac, M.; Mulvey, R. E. Alkali-Metal-Mediated Synergistic Effects in Polar Main Group Organometallic Chemistry. *Chem. Rev.* **2019**, *119*, 8332. (c) McLellan, R.; Uzelac, M.; Bole, L. J.; Gil-Negrete, J. M.; Armstrong, D. R.; Kennedy, A. R.; Mulvey, R. E.; Hevia, E. Alkali Metal Effects in Trans-Metal-Trapping (TMT): Comparing LiTMP with NaTMP in Cooperative MTMP/Ga-$(CH_2SiMe_3)_3$ Metalation Reactions. *Synthesis* **2019**, *51*, 1207. (d) Garden, J. A.; Armstrong, D. R.; Clegg, W.; Garcia-Alvarez, J.; Hevia, E.; Kennedy, A. R.; Mulvey, R. E.; Robertson, S. D.; Russo, L. Donor-Activated Lithiation and Sodiation of Trifluoromethylbenzene: Structural, Spectroscopic, and Theoretical Insights. *Organometallics* **2013**, *32*, 5481. (e) Wong, H. C. Is Sodium Finally Coming of Age? *Nature Catal.* **2019**, *2*, 282.

(7) (a) Seyferth, D. Alkyl and Aryl Derivatives of the Alkali Metals: Useful Synthetic Reagents as Strong Bases and Potent Nucleophiles. 1. Conversion of Organic Halides to Organoalkali-Metal Compounds. *Organometallics* **2006**, *25*, 2. (b) Seyferth, D. Alkyl and Aryl Derivatives of the Alkali Metals: Strong Bases and Reactive Nucleophiles. 2. Wilhelm Schlenk's Organoalkali-Metal Chemistry. The Metal Displacement and the Transmetalation Reactions. Metalation of Weakly Acidic Hydrocarbons. Superbases. *Organometallics* **2009**, *28*, 2. (c) Benkeser, R. A.; Foster, D. J.; Sauve, D. M.; Nobis, J. F. Metalations With Organosodium Compounds. *Chem. Rev.* **1957**, *57*, 867. (d) Schlosser, M. In *Organometallics in Synthesis: A Manual*, 2nd ed.; Schlosser, M., Ed.; John Wiley & Sons: Chichester, 2002; Chapter 1. (e) Langer, A. W., Jr., Ed. *Polyamine-Chelated Alkali Metal Compounds*; American Chemical Society: Washington, DC, 1974. (f) Szwarc, M., Ed. *Ions and Ion Pairs in Organic Reactions*; Wiley: New York, 1972; Vols. 1 and 2. (g) Szwarc, M. *Carbanions, Living Polymers, and Electron-Transfer Processes*; Interscience: New York, 1968.

(8) For a review of the structural, mechanistic, and synthetic applications of NaDA, see: Woltornist, R. A.; Ma, Y.; Algera, R. F.; Zhou, Y.; Zhang, Z.; Collum, D. B. Structure, Reactivity, and Synthetic Applications of Sodium Diisopropylamide. *Synthesis* **2020**, *52*, 1478.

(9) (a) Schade, C.; Bauer, W.; Von Ragué Schleyer, P. *n*-Butylsodium: The Preparation, Properties and NMR Spectra of a Hydrocarbon- and Tetrahydrofuran-Soluble Reagent. *J. Organomet. Chem.* **1985**, *295*, c25. (b) Turner, R. R.; Altenau, A. G.; Cheng, T. C. Analysis of Butyllithium and Butylsodium in the Presence of Alkoxides. *Anal. Chem.* **1970**, *42*, 1835. (c) Majewski, S., Ed. Product Subclass 9: Allylsodium Compounds. In *Category 1, Organometallics*; Georg Thieme Verlag: Stuttgart, 2016. (d) Lochmann, L.; Pospíšil, J.; Lím, D. On the Interaction of Organolithium Compounds with Sodium and Potassium Alkoxides. A New Method for the Synthesis of Organosodium and Organopotassium Compounds. *Tetrahedron Lett.* **1966**, *7*, 257. (e) Hill, M. S.; Hitchcock, P. B. Sodium and Potassium Derivatives of Diphenyl(trimethylsilyl)methane. *J. Organomet. Chem.* **2002**, *664*, 182. (f) Harenberg, J. H.; Weidmann, N.; Wiegand, A. J.; Hoefer, C. A.; Annapureddy, R. R.; Knochel, P. (2-Ethylhexyl)-sodium: A Hexane-Soluble Reagent for Br/Na-Exchanges and Directed Metalations in Continuous Flow. *Angew. Chem., Int. Ed.* **2021**, *60*, 14296.

(10) We examined the efficacy of 2-ethylhexylsodium as a hydrocarbon soluble alkylsodium and found it functional but inconvenient to manipulate: (a) Arest-Yakubovich, A. A.; Nakhmanovich, B. I.; Litvinenko, G. I. *Polymer* **2002**, *43*, 7093. (b) Maréchal, J.-M.; Carlotti, S.; Shcheglova, L.; Deffieux, A. *Polymer* **2003**, *44*, 7601.

(11) For recent progress in preparing and using NaTMP, see the following (and references cited therein): Asako, S.; Kodera, M.; Nakajima, H.; Takai, K. Lithium-Free Synthesis of Sodium 2, 2, 6, 6-Tetramethylpiperidide and Its Synthetic Applications. *Adv. Synth. Catal.* **2019**, *361*, 3120.

(12) (a) Ma, Y.; Algera, R. F.; Collum, D. B. Sodium Diisopropylamide in *N,N*-Dimethylethylamine: Reactivity, Selectivity, and Synthetic Utility. *J. Org. Chem.* **2016**, *81*, 11312. (b) Algera, R. F.; Ma, Y.; Collum, D. B. Sodium Diisopropylamide: Aggregation, Solvation, and Stability. *J. Am. Chem. Soc.* **2017**, *139*, 7921. (c) Algera, R. F.; Ma, Y.; Collum, D. B. Sodium Diisopropylamide in Tetrahydrofuran: Selectivities, Rates, and Mechanisms of Alkene and Diene Isomerizations and Metalations. *J. Am. Chem. Soc.* **2017**, *139*, 11544. (d) Ma, Y.; Woltornist, R. A.; Algera, R. F.; Collum, D. B. Mechanisms of Orthosodiations and Snieckus-Fries Rearrangements. *J. Org. Chem.* **2019**, *84*, 9051. (e) Ma, Y.; Algera, R. F.; Woltornist, R. A.; Collum, D. B. Sodium Diisopropylamide-Mediated Dehydrohalogenations: Influence of Primary- and Secondary-Shell Solvation. *J. Org. Chem.* **2019**, *84*, 10860.

(13) Han, Z.; Chen, S.; Tu, Y.; Lian, X.; Li, G. Fluoroform: An Efficient Precursor for the Trifluoromethylation of Aromatic Esters by Sodium Diisopropylamide with Trialkylamines. *Eur. J. Org. Chem.* **2019**, *2019*, 4658.

(14) Mordini, A. Sodium and Potassium. In *Comprehensive Organometallic Chemistry III*; Mingos, D. M. P., Crabtree, R. H., Eds; Elsevier, 2007; Vol. *9*, p 3.

(15) (a) Jost, S.; Günther, H. ^{13}C and ^{23}Na Solid-State NMR Spectra of Organosodium Compounds. *Magn. Reson. Chem.* **2003**, *41*, 373. (b) McMillen, H.; Gren, C. K.; Hanusa, T. P.; Rheingold, A. L. A Tetrameric Allyl Complex of Sodium, and Computational Modeling of the $^{23}Na-Allyl$ Chemical Shift. *Inorg. Chim. Acta* **2010**, *364*, 61. (c) Pakuro, N. I.; Arest-Yakubovich, A. A.; Shcheglova, L. V.; Petrovsky, P. V.; Chekulaeva, L. A. NMR Spectra of a Hydrocarbon-Soluble Organosodium Compound and Its Lithium Analogs. *Russ. Chem. Bull.* **1996**, *45*, 838. (d) Delville, A.; Detellier, C.; Gerstmans, A.; Laszlo, P. Chelation of the Sodium Cation by Polyamines: A Novel Approach to Preferential Solvation, and to the Understanding of Sodium-23 Chemical Shifts and Quadrupolar Coupling Constants. *J. Am. Chem. Soc.* **1980**, *102*, 6558. (e) Boche, G.; Etzrodt, H. The Reaction of *n*-Butyllithium/sodium(potassium) *tert*-Butoxide (Lochmann-Schlosser Base) with a CH-Acid Leads to Organosodium-(potassium) Compounds. An NMR Spectroscopical Study of Several Organolithium, -sodium and -potassium Compounds in Tetrahydrofuran-d_8. *Tetrahedron Lett.* **1983**, *24*, 5477.

(16) (a) Nakhmanovich, B. I.; Zolotareva, I. V.; Litvinenko, G. I.; Arest-Yakubovich, A.; Muller, A. H. E. Anionic Polymerization of Butadiene Initiated by Tributyltin Sodium. Kinetic Analysis of Induction Periods Generated by Transfer to Initiator Precursor *Macromolec. Macromol. Chem. Phys.* **2001**, *202*, 3536. (b) Alvarino, J. M. Structure of the Ionic Species in Organosodium Compounds Dissolved in n-Electron Donor, Low Dielectric Constant Media. *J. Organomet. Chem.* **1975**, *90*, 133. (c) Ahlberg, P.; Karlsson, A.; Davidsson, O.; Hilmersson, G.; Loewendahl, M. Mechanism and Solvent Catalysis of the Degenerate 1,12-Metalations of [1.1]-Ferrocenophanyllithium and [1.1]Ferrocenophanylsodium Studied by NMR Spectroscopy. *J. Am. Chem. Soc.* **1997**, *119*, 1751.

(17) Schleyer, P. v. R.; Clark, T.; Kos, A. J.; Spitznagel, G. W.; Rohde, C.; Arad, D.; Houk, K. N.; Rondan, N. G. Structures and Stabilities of α-Hetero-Substituted Organolithium and Organosodium Compounds. Energetic Unimportance of Second-Row d-Orbital Effects. *J. Am. Chem. Soc.* **1984**, *106*, 6467. (b) Papadopoulos, M. G.; Raptis, S. G.; Demetropoulos, I. N. Organolithium and Organosodium compounds: the Second Hyperpolarizabilities of $C_8H_6Li_2$ and $C_8H_6Na_2$. *Mol. Phys.* **1997**, *92*, 547. (c) Sabirov, Z. M.; Manakov, Yu. B.; Ponomarev, O. A.; Minsker, K. S.; Rafikov, S. R. Theoretical Study of the Structure and Reactivity of Active Centers During Anionic Polymerization of Unsaturated Nonpolar Monomers. *Zh. Fiz. Khim.* **1985**, *59*, 1136. (d) Sulway, S. A.; Girshfeld, R.; Solomon, S. A.; Muryn, C. A.; Poater, J.; Solà, M.; Bickelhaupt, F. M.; Layfield, R. A. Alkali Metal Complexes of Silyl-Substitutedansa-(Tris)allyl Ligands: Metal-, Co-Ligand-, and Substituent-Dependent Stereochemistry. *Eur. J. Inorg. Chem.* **2009**, *2009*, 4157. (e) Majhi, J.; Turnbull, B. W. H.; Ryu, H.; Park, J.; Baik, M.-H.; Evans, P. A. Dynamic Kinetic Resolution of Alkenyl Cyanohydrins Derived from

https://doi.org/10.1021/jacs.1c06528
J. Am. Chem. Soc. 2021, 143, 13370−13381

α,β-Unsaturated Aldehydes: Stereoselective Synthesis of E-Tetrasubstituted Olefins. *J. Am. Chem. Soc.* **2019**, *141*, 11770.
(18) Collum, D. B.; McNeil, A. J.; Ramírez, A. Lithium Diisopropylamide: Solution Kinetics and Implications for Organic Synthesis. *Angew. Chem., Int. Ed.* **2007**, *46*, 3002.
(19) Studies of base-mediated solvent decomposition: (a) Holm, T. Association of Butyllithium in Diethyl Ether and in Tetrahydrofuran. *Acta Chem. Scand.* **1978**, *32B*, 162. (b) Bates, T. F.; Clarke, M. T.; Thomas, R. D. Unusual Stability of an Alkyllithium Dimer: Preparation, Properties, and Decomposition Mechanism of *tert*-Butyllithium Dietherate Dimer. *J. Am. Chem. Soc.* **1988**, *110*, 5109. (c) Raposo, M. L.; Fernández-Nieto, F.; Garcia-Rio, L.; Rodríguez-Dafonte, P.; Paleo, M. R.; Sardina, F. J. Mechanism of the Deprotonation Reaction of Alkyl Benzyl Ethers with *n*-Butyllithium. *Chem. - Eur. J.* **2013**, *19*, 9677. (d) Corset, J.; Castellà-Ventura, M.; Froment, F.; Strzalko, T.; Wartski, L. Formation Mechanism of Acetaldehyde Lithium Enolate by Reaction of *n*-Butyllithium with Tetrahydrofuran: Infrared and Raman Spectroscopy and Density Functional Theory Calculations. *J. Raman Spectrosc.* **2002**, *33*, 652. (e) Also, see ref 12b.
(20) The potential merits of simple trialkylamines in organosodium chemistry were foreshadowed decades ago with studies of amylsodium in triethylamine: (a) Morton, A. A.; Ward, F. K. The Effect of Triethylamine on the Decomposition of Amylsodium. *J. Org. Chem.* **1960**, *25*, 120. (b) Gilman, H.; Bebb, R. L. Relative Reactivities of Organometallic Compounds. XX. Metalation. *J. Am. Chem. Soc.* **1939**, *61*, 109.
(21) For early studies revealing the poor coordination of trialkylamines to organolithium aggregates, see: (a) Settle, F. A.; Haggerty, M.; Eastham, J. F. High Frequency Titrimetric Determination of the Electron Deficiency in Lithium Alkyls. *J. Am. Chem. Soc.* **1964**, *86*, 2076. (b) Lewis, H. L.; Brown, T. L. Association of Alkyllithium Compounds in Hydrocarbon Media. Alkyllithium-Base Interactions. *J. Am. Chem. Soc.* **1970**, *92*, 4664. (c) Brown, T. L.; Gerteis, R. L.; Rafus, D. A.; Ladd, J. A. Interaction of Alkyllithium Compounds with Base. Complex Formation between Ethyllithium and Triethylamine in Benzene. *J. Am. Chem. Soc.* **1964**, *86*, 2135. (d) Quirk, R. P.; Kester, D. E. The Rates of Monometallation of Alkylphenylacetylenes. *J. Organomet. Chem.* **1977**, *127*, 111.
(22) (a) Corbelin, S.; Kopf, J.; Weiss, E. Monomeres, Tetrameres und Polymeres Natriumfluorenid-S [S = $Me_2N(CH_2)_2N(Me)(CH_2)_2NMe_2$, $Me_2N(CH_2)_nNMe_2$ (*n* = 2, 3)]. *Chem. Ber.* **1991**, *124*, 2417. (b) Comins, D. L.; Brown, J. D. Orthometalation Directed by.alpha.-Amino Alkoxides. *J. Org. Chem.* **1984**, *49*, 1078. (c) Andrews, P. C.; Koutsaplis, M.; Robertson, E. G. Thermodynamically Favored Anion Rearrangements in Li and Na Complexes of (S)-N-α-(Methylbenzyl)allylamine. *Organometallics* **2009**, *28*, 1697. (d) Andrews, P. C.; Blair, V. L.; Koutsaplis, M.; Thompson, C. D. Anion Rearrangements of Alkali Metal Complexes of the Chiral Amine (*S*)-N-α-(Methylbenzyl)phenylallylamine: Structural and Solution Insights. *Organometallics* **2012**, *31*, 8135.
(23) (a) Koehler, F. H.; Hertkorn, N.; Bluemel, J. Die Metallierung von *N,N,N′,N′*-Tetramethylethylendiamin (TMEDA). *Chem. Ber.* **1987**, *120*, 2081. (b) Conway, B.; García-Álvarez, J.; Hevia, E.; Kennedy, A. R.; Mulvey, R. E.; Robertson, S. D. Contacted Ion-Pair Lithium Alkylamidoaluminates. Intramolecular Alumination (Al-H Exchange) Traps for TMEDA and PMDETA. *Organometallics* **2009**, *28*, 6462. (c) Klumpp, G. W.; Luitjes, H.; Schakel, M.; de Kanter, F. J. J.; Schmitz, R. F.; van Eikema Hommes, N. J. R. *N*-Lithiomethyl-*N,N′,N′,N″*-tetramethyldiethylenetriamine: The First Alkyllithium Compound which is Monomeric in Hydrocarbons. *Angew. Chem., Int. Ed. Engl.* **1992**, *31*, 633. (d) Luitjes, H.; Schakel, M.; Aarnts, M. P.; Schmitz, R. F.; de Kanter, F. J. J.; Klumpp, G. W. Reactions of the Butyllithiums with Tertiary Oligoethylenepolyamines. *Tetrahedron* **1997**, *53*, 9977. (e) Wang, Y.; Liu, J.; Huang, L.; Zhu, R.; Huang, X.; Moird, R.; Huang, J. KO-*t*-Bu-Catalyzed Lithiation of PMDTA and the Direct Functionalization of Bridged Alkenes Ander Mild Conditions. *Chem. Commun.* **2017**, *53*, 4589.
(24) Collum, D. B. Is *N,N,N′,N′*-Tetramethylethylenediamine a Good Ligand for Lithium? *Acc. Chem. Res.* **1992**, *25*, 448.
(25) (a) Frausto da Silva, J. J. R. The Chelate Effect Redefined. *J. Chem. Educ.* **1983**, *60*, 390. (b) Simmons, E. L. More on the Chelate Effect. *J. Chem. Educ.* **1979**, *56*, 578.
(26) The most common use of hemilability appears to involve polyfunctional ligands in which one portion is weakly bound, presumably mitigating the costs of chelate scission to provide access to a coordination site. For reviews of hemilabile ligands, see: (a) Braunstein, P.; Naud, F. Hemilability of Hybrid Ligands and the Coordination Chemistry of Oxazoline-Based Systems. *Angew. Chem., Int. Ed.* **2001**, *40*, 680. (b) Miller, A. J. M. Controlling Ligand Binding for Tunable and Switchable Catalysis: Cation-Modulated Hemilability in Pincer-Crown Ether Ligands. *Dalt. Trans.* **2017**, *46*, 11987. (c) Annibale, V. T.; Song, D. Multidentate Actor Ligands as Versatile Platforms for Small Molecule Activation and Catalysis. *RSC Adv.* **2013**, *3*, 11432.
(27) Ramírez, A.; Sun, X.; Collum, D. B. Lithium Diisopropylamide-Mediated Enolization: Catalysis by Hemilabile Ligands. *J. Am. Chem. Soc.* **2006**, *128*, 10326.
(28) For discussions of the challenges of ligand-catalyzed organolithium reactions, see: Kizirian, J.-C. Chiral Tertiary Diamines in Asymmetric Synthesis. *Chem. Rev.* **2008**, *108*, 140.
(29) (a) Steffen, P.; Unkelbach, C.; Christmann, M.; Hiller, W.; Strohmann, C. Catalytic and Stereoselective Ortho-Lithiation of a Ferrocene Derivative. *Angew. Chem., Int. Ed.* **2013**, *52*, 9836. (b) Gammon, J. J.; Canipa, S. J.; O'Brien, P.; Kelly, B.; Taylor, S. Catalytic Asymmetric Deprotonation of Phosphine Boranes and Sulfides as a Route to P-Stereogenic Compounds. *Chem. Commun.* **2008**, 3750.
(30) (a) Denmark, S. E.; Nakajima, N.; Nicaise, O. J.-C. Asymmetric Addition of Organolithium Reagents to Imines. *J. Am. Chem. Soc.* **1994**, *116*, 8797. (b) Desimoni, G.; Faita, G.; Jørgensen, K. A. C_2-Symmetric Chiral *Bis*(oxazoline) Ligands in Asymmetric Catalysis. *Chem. Rev.* **2011**, *111*, PR284. (c) Denmark, S. E.; Nakajima, N.; Stiff, C. M.; Nicaise, O. J.-C.; Kranz, M. Studies on the Bisoxazoline and (−)-Sparteine-Mediated Enantioselective Addition of Organolithium Reagents to Imines. *Adv. Synth. Catal.* **2008**, *350*, 1023.
(31) For reviews on phase-transfer catalysis, see: (a) Naik, S. D.; Doraiswamy, L. K. Phase Transfer Catalysis: Chemistry and Engineering. *AIChE J.* **1998**, *44*, 612. (b) Dehmlow, E. V.; Dehmlow, S. S. *Phase Transfer Catalysis*, 3rd ed.; VCH: Weinheim, 1993. (c) Starks, C. M.; Liotta, C. L.; Halpern, M. *Phase-Transfer Catalysis*; Chapman & Hall: New York, 1994. (d) Sasson, Y.; Neumann, R. *Handbook of Phase-Transfer Catalysis*; Blackie Academic & Professional: London, 1997. (e) Halpern, M. E. *Phase-Transfer Catalysis*; ACS Symposium Series 659; American Chemical Society: Washington DC, 1997. (f) Tan, J.; Yasuda, N. Contemporary Asymmetric Phase Transfer Catalysis: Large-Scale Industrial Applications. *Org. Process Res. Dev.* **2015**, *19*, 1731.
(32) Liotta, C. L.; Berkner, J.; Wright, J.; Fair, B. Mechanisms and Applications of Solid—Liquid Phase-Transfer Catalysis. In *Phase-Transfer Catalysis*; Halpern, M., Ed.; ACS Symposium Series; American Chemical Society: Washington, DC, 1997.
(33) A search of the chemical literature at the time of writing afforded 167 reports of solid−liquid phase-transfer catalysis.
(34) (a) Phipps, R. J.; Toste, F. D. Chiral Anion Phase-Transfer Catalysis Applied to the Direct Enantioselective Fluorinative Dearomatization of Phenols. *J. Am. Chem. Soc.* **2013**, *135*, 1268. (b) Xia, Z.-L.; Xu-Xu, Q.-F.; Zheng, C.; You, S.-L. Chiral Phosphoric Acid-Catalyzed Asymmetric Dearomatization Reactions. *Chem. Soc. Rev.* **2020**, *49*, 286.
(35) (a) Perrard, T.; Plaquevent, J.-C.; Desmurs, J. R.; Hébrault, D. Enantioselective Synthesis of Both Enantiomers of Methyl Dihydrojasmonate Using Solid-Liquid Asymmetric Phase-Transfer Catalysis. *Org. Lett.* **2000**, *2*, 2959. (b) Loupy, A.; Sansoulet, J.; Zaparucha, A.; Merienne, C. Solid-Liquid Phase Transfer Catalysis Without Solvent: An Improvement for Chiral Michael Addition of *N*-Acetylaminohalonate to Chalcone. *Tetrahedron Lett.* **1989**, *30*, 333.

https://doi.org/10.1021/jacs.1c06528
J. Am. Chem. Soc. 2021, 143, 13370−13381

(c) Loupy, A.; Zaparucha, A. Asymmetric Michael Reaction Under PTC Conditions Without Solvent Importance of π interactions for the Enantioselectivity. *Tetrahedron Lett.* **1993**, *34*, 473. (d) Mirza-Aghayan, M.; Etemad-Moghadam, G.; Zaparucha, A.; Berlan, J.; Loupy, A.; Koenig, M. Ultrasound Irradiation Effects on the Asymmetric Michael Reaction. *Tetrahedron: Asymmetry* **1995**, *6*, 2643. (e) Nowicki, A.; Keldenich, J.; Agbossou-Niedercorn, F. Highly Selective Preparation of a Chiral Quaternary Allyl Aryl Piperidine-dione by Palladium-Catalyzed Asymmetric Allylation Under Solid−Liquid Phase-Transfer Catalysis. *Eur. J. Org. Chem.* **2007**, *2007*, 6124. (f) Foschi, F.; Albanese, D.; Pecnikaj, I.; Tagliabue, A.; Penso, M. Regioselective O-Sulfonylation of *N, N*- Bis(2-hydroxyalkyl) tosylamides as a Synthetic Key Step to Enantiopure Morpholines. *Org. Lett.* **2017**, *19*, 70.

(36) For reviews and leading references to asymmetric phase-transfer catalysis, see: (a) Shirakawa, S.; Maruoka, K. Recent Developments in Asymmetric Phase-Transfer Reactions. *Angew. Chem., Int. Ed.* **2013**, *52*, 4312. (b) Ooi, T.; Maruoka, K. Recent Advances in Asymmetric Phase-Transfer Catalysis. *Angew. Chem., Int. Ed.* **2007**, *46*, 4222. (c) Shirakawa, S.; Maruoka, K. Asymmetric phase-transfer reactions under base-free neutral conditions. *Tetrahedron Lett.* **2014**, *55*, 3833. (d) Dolling, U. H.; Davis, P.; Grabowski, E. J. J. Efficient Catalytic Asymmetric Alkylations. 1. Enantioselective Synthesis of (+)-Indacrinone via Chiral Phase-Transfer Catalysis. *J. Am. Chem. Soc.* **1984**, *106*, 446. (e) O'Donnell, M. J. The Preparation of Optically Active alpha-Amino Acids from the Benzophenone Imines of Glycine Derivatives. *Aldrichimica Acta* **2001**, *34*, 3. (f) Maruoka, K.; Ooi, T. Enantioselective Amino Acid Synthesis by Chiral Phase-Transfer Catalysis. *Chem. Rev.* **2003**, *103*, 3013. (g) O'Donnell, M. J. The Enantioselective Synthesis of α-Amino Acids by Phase-Transfer Catalysis with Achiral Schiff Base Esters. *Acc. Chem. Res.* **2004**, *37*, 506. (h) Also, see ref 30.

(37) Sirovski, F.; Reichardt, R.; Gorokhova, M.; Ruban, S.; Stoikova, E. Solid/Liquid Phase-Transfer Catalysis. Some Models and Solvent Influence. *Tetrahedron* **1999**, *55*, 6363.

(38) (a) Kano, T.; Aota, Y.; Maruoka, K. Rate Acceleration of Solid-Liquid Phase-Transfer Catalysis by Rotor-Stator Homogenizer. *Adv. Synth. Catal.* **2016**, *358*, 2996. (b) Sasson, Y.; Bilman, N. Mechanism of Solid/Liquid Phase-transfer Catalysis in the Presence of Potassium Carbonate: Alkylation of Pyrrolidin-2-one. *J. Chem. Soc., Perkin Trans. 2* **1989**, 2029.

(39) Yadav, G. D.; Bisht, P. M. Novelties of Microwave Irradiated Solid-Liquid Phase Transfer Catalysis (MISL-PTC) in Synthesis of 2′-Benzyloxyacetophenone. *J. Mol. Catal. A: Chem.* **2004**, *221*, 59.

(40) Anderson, N. G. *Practical Process Research and Development - A Guide For Organic Chemists*, 2nd ed.; Academic Press: New York, 2012.

(41) (a) Rein, A. J.; Donahue, S. M.; Pavlosky, M. A. In Situ FTIR Reaction Analysis of Pharmaceutical-Related Chemistry and Processes. *Curr. Opin. Drug Discovery Dev.* **2000**, *3*, 734. (b) Defernez, M.; Wilson, R. H. Infrared Spectroscopy: Instrumental Factors Affecting the Long-Term Validity of Chemometric Models. *Anal. Chem.* **1997**, *69*, 1288. (c) Brodmann, T.; Koos, P.; Metzger, A.; Knochel, P.; Ley, S. V. Continuous Preparation of Arylmagnesium Reagents in Flow with Inline IR Monitoring. *Org. Process Res. Dev.* **2012**, *16*, 1102. (d) Connolly, T. J.; Hansen, E. C.; MacEwan, M. F. In Situ FTIR Study and Scale-Up of an Enolization-Azidation Sequence. *Org. Process Res. Dev.* **2010**, *14*, 466.

(42) Whereas all PMDTA-catalyzed rates in DMEA vs DEMA are related by a constant related to their relative binding constants, the basal rates include differential binding of the simple trialkyamines in the transition states, which leads to mechanism-dependent values of k_{rel} for the two cosolvents.

(43) Previous rate studies have revealed mechanistic details for the NaDA/THF-mediated metalations in Table 1, entries 2, 5−7, 14, and 18.[8,12]

(44) (a) Barry, J.; Bram, G.; Decodts, G.; Loupy, A.; Pigeon, P.; Sansoulet, J. Solid-Liquid Phase-Transfer Catalysis Reactions without Solvent; Very Mild Conditions for β-eliminations. *J. Org. Chem.* **1984**, *49*, 1138. (b) Wolkoff, P. Dehydrobromination of Secondary and Tertiary Alkyl and Cycloalkyl Bromides with 1,8-Diazabicyclo[5.4.0]-undec-7-ene. Synthetic Applications. *J. Org. Chem.* **1982**, *47*, 1944.

(45) Bertilsson, S. K.; Södergren, M. J.; Andersson, P. G. New Catalysts for the Base-Promoted Isomerization of Epoxides to Allylic Alcohols. Broadened Scope and Near-Perfect Asymmetric Induction. *J. Org. Chem.* **2002**, *67*, 1567.

(46) Mordini, A. Facile Isomerization of Oxiranes to Allyl Alcohols by Mixed Metal Bases. *Tetrahedron* **1990**, *46*, 2401.

(47) Singh, K. J.; Collum, D. B. Lithium Diisopropylamide-Mediated Ortholithiation and Anionic Fries Rearrangement of Aryl Carbamates: Role of Aggregates and Mixed Aggregates. *J. Am. Chem. Soc.* **2006**, *128*, 13753.

(48) (a) Woltornist, R. A.; Collum, D. B. Using $^{15}N-^{29}Si$ Scalar Coupling to Determine Aggregation and Solvation States. *J. Am. Chem. Soc.* **2020**, *142*, 6852. (b) Woltornist, R. A.; Collum, D. B. Aggregation and Solvation of Sodium Hexamethyldisilazide Across the Solvent Spectrum. *J. Org. Chem.* **2021**, *86*, 2406.

(49) Extensive review of structural studies of alkali metal mixed aggregates: Harrison-Marchand, A.; Mongin, F. Mixed Aggregate (MAA): A Single Concept for All Dipolar Organometallic Aggregates. 1. Structural Data. *Chem. Rev.* **2013**, *113*, 7470. Also, see ref 6a.

(50) Kennedy, A. R.; Mulvey, R. E.; Urquhart, R. I.; Robertson, S. D. Lithium, Sodium and Potassium Picolyl Complexes: Syntheses, Structures and Bonding. *Dalton Trans.* **2014**, *43*, 14265.

(51) Casado, J.; Lopez-Quintela, M. A.; Lorenzo-Barral, F. M. The Initial Rate Method in Chemical Kinetics: Evaluation and Experimental Illustration. *J. Chem. Educ.* **1986**, *63*, 450.

(52) The data at early conversion is fitted to a third-order polynomial (at^2+bt+c) making sure not to include too much curvature. The parameter b represents the rate at time zero. (One may verify this by taking the first derivative with respect to t and setting $t = 0$. Initial rate = $f'(0) = b$.)

(53) We make two approximations to keep the fit relatively simple. First, the contribution from the basal metalation rate in DMEA is quite small but not a constant as the increasing PMDTA concentrations displace the coordinated DMEA. Second, we include no provisions for contributions from a DMEA−PMDTA mixed solvate, which is justified by the absence of curvatures in the data at low PMDTA contributions.

(54) A number of general-purpose reviews on determining reaction mechanism: (a) Meek, S. J.; Pitman, C. L.; Miller, A. J. M. Deducing Reaction Mechanism: A Guide for Students, Researchers, and Instructors. *J. Chem. Educ.* **2016**, *93*, 275. (b) Simmons, E. M.; Hartwig, J. F. On the Interpretation of Deuterium Kinetic Isotope Effects in C−H Bond Functionalizations by Transition Metal Complexes. *Angew. Chem., Int. Ed.* **2012**, *51*, 3066. (c) Algera, R. F.; Gupta, L.; Hoepker, A. C.; Liang, J.; Ma, Y.; Singh, K. J.; Collum, D. B. Lithium Diisopropylamide: Non-Equilibrium Kinetics and Lessons Learned about Rate Limitation. *J. Org. Chem.* **2017**, *82*, 4513. (d) See also ref 18.

(55) Frisch, M. J.; Trucks, G. W.; Schlegel, H. B.; Scuseria, G. E.; Robb, M. A.; Cheeseman, J. R.; Scalmani, G.; Barone, V.; Mennucci, B.; Petersson, G. A.; Nakatsuji, H.; Caricato, M.; Li, X.; Hratchian, H. P.; Izmaylov, A. F.; Bloino, J.; Zheng, G.; Sonnenberg, J. L.; Hada, M.; Ehara, M.; Toyota, K.; Fukuda, R.; Hasegawa, J.; Ishida, M.; Nakajima, T.; Honda, Y.; Kitao, O.; Nakai, H.; Vreven, T.; Montgomery, J. A., Jr.; Peralta, J. E.; Ogliaro, F.; Bearpark, M.; Heyd, J. J.; Brothers, E.; Kudin, K. N.; Staroverov, V. N.; Kobayashi, R.; Normand, J.; Raghavachari, K.; Rendell, A.; Burant, J. C.; Iyengar, S. S.; Tomasi, J.; Cossi, M.; Rega, N.; Millam, J. M.; Klene, M.; Knox, J. E.; Cross, J. B.; Bakken, V.; Adamo, C.; Jaramillo, J.; Gomperts, R.; Stratmann, R. E.; Yazyev, O.; Austin, A. J.; Cammi, R.; Pomelli, C.; Ochterski, J. W.; Martin, R. L.; Morokuma, K.; Zakrzewski, V. G.; Voth, G. A.; Salvador, P.; Dannenberg, J. J.; Dapprich, S.; Daniels, A. D.; Farkas, O.; Foresman, J. B.; Ortiz, J. V.; Cioslowski, J.; Fox, D. J. *Gaussian 09*, revision A.02; Gaussian, Inc.: Wallingford, CT, 2009.

(56) Zhao, Y.; Truhlar, D. G. The M06 Suite of Density Functionals for Main Group Thermochemistry, Thermochemical Kinetics,

https://doi.org/10.1021/jacs.1c06528
J. Am. Chem. Soc. 2021, 143, 13370−13381

Noncovalent Interactions, Excited States, and Transition Elements: Two New Functionals and Systematic Testing of Four M06-Class Functionals and 12 Other Functionals. *Theor. Chem. Acc.* **2008**, *120*, 215.
(57) Weigend, F.; Ahlrichs, R. Balanced Basis Sets of Split Valence, Triple Zeta Valence and Quadruple Zeta Valence Quality for H to Rn: Design and Assessment of Accuracy. *Phys. Chem. Chem. Phys.* **2005**, *7*, 3297.
(58) Legault, C. Y. *CYLview—Visualization and Analysis Software for Computational Chemistry*. http://www.cylview.org (accessed 2021-07-23).
(59) We define the idealized rate law as that obtained by rounding the observed reaction orders to the nearest rational order.
(60) Moore, J. W.; Pearson, R. G. *Kinetics and Mechanism*, 3rd ed.; Wiley, New York, 1981; p 60.
(61) (a) Briggs, T. F.; Winemiller, M. D.; Collum, D. B.; Parsons, R. L., Jr.; Davulcu, A. K.; Harris, G. D.; Fortunak, J. D.; Confalone, P. N. Structural and Rate Studies of the 1,2-Additions of Lithium Phenylacetylide to Lithiated Quinazolinones: Influence of Mixed Aggregates on the Reaction Mechanism. *J. Am. Chem. Soc.* **2004**, *126*, 5427. (b) Ma, Y.; Breslin, S.; Keresztes, I.; Lobkovsky, E.; Collum, D. B. Synthesis of 7-Azaindoles by Chichibabin Cyclization: Reversible Base-Mediated Dimerization of 3-Picolines. *J. Org. Chem.* **2008**, *73*, 9610.
(62) Rutherford, J. L.; Hoffmann, D.; Collum, D. B. Consequences of Correlated Solvation on the Structures and Reactivities of RLi-Diamine Complexes: 1,2-Addition and α-Lithiation Reactions of Imines by TMEDA-Solvated *n*-Butyllithium and Phenyllithium. *J. Am. Chem. Soc.* **2002**, *124*, 264.
(63) Given equal enthalpic affinities of L for A_2S_2 and A_2LS (eq 8), $K_1 = 4K_2$ owing to purely statistical contributions. For the proper treatment of such factors, see: (a) Benson, S. W. Statistical Factors in the Correlation of Rate Constants and Equilibrium Constants. *J. Am. Chem. Soc.* **1958**, *80*, 5151. For additional leading references to statistical contributions in "redistribution reactions", see: (b) Fay, R. C.; Lowry, R. N. Proton Magnetic Resonance Studies of Ligand-Exchange Equilibriums for Dihalo- and Diethoxybis(.beta.-diketonato)titanium(IV) Complexes. *Inorg. Chem.* **1974**, *13*, 1309.
(64) Although one could imagine that trace decomposition of NaDA via NaH then provides an imine that could provide up to 12 protons from the isopropyl. We have seen no evidence of this in multiple studies of using NaDA/THF.[18] Alternatively, reversible metalation of PMDTA[23] has precedent. We did not pursue this issue further.
(65) Preparations of 1,1-**1**-d_2 and 2,2-**1**-d_2: Boden, N.; Bushby, R. J.; Clark, L. D. The Synthesis of Specifically and Selectively Deuteriated 4,4′- Bisalkoxyazoxybenzene Derivatives. *J. Chem. Soc., Perkin Trans. 1* **1983**, 543.
(66) The concentration of the NaDA, although expressed in units of molarity, refers to the concentration of the monomer unit (normality).
(67) A brief investigation of the elimination of cyclooctene oxide **15** with NaDA/hexane in the absence of catalyst reveals a nearly zeroth-order dependence on epoxide concentration (Supporting Information). Whether that implicates a rate-limiting dissociation of NaDA from a surface-saturated solid NaDA or reaction of the NaDA at the surface, the quality of the data was a bit surprising.
(68) Ramírez, A.; Collum, D. B. LDA mediated formation of bicyclic alcohol Hemilabile Ligands in Organolithium Chemistry: Rate Studies of the LDA-Mediated α- and β-Metalations of Epoxides. *J. Am. Chem. Soc.* **1999**, *121*, 11114.
(69) For NaHMDS—sodium enolate mixed aggregates, see: (a) Williard, P. G.; Hintze, M. J. Mixed Aggregates: Crystal Structures of a Lithium Ketone Enolate/Lithium Amide and of a Sodium Ester Enolate/Sodium Amide. *J. Am. Chem. Soc.* **1990**, *112*, 8602. (b) Zhang, Z.; Collum, D. B. Structures and Reactivities of Sodiated Evans Enolates: Role of Solvation and Mixed Aggregation on the Stereochemistry and Mechanism of Alkylations. *J. Am. Chem. Soc.* **2019**, *141*, 388. (c) Ojeda-Amador, A. I.; Martinez-Martinez, A. J.; Kennedy, A. R.; O'Hara, C. T. Synthetic and Structural Studies of Mixed Sodium bis(Trimethylsilyl) Amide/Sodium Halide Aggregates in the Presence of η^2-*N,N*-, η^3-*N,N,N/N,O,N*-, and η^4-*N,N,N,N*-Donor Ligands. *Inorg. Chem.* **2015**, *54*, 9833.
(70) McSweeney, C. M.; Foley, V. M.; McGlacken, G. P. The Asymmetric Alkylation of Dimethylhydrazones; Intermolecular Chirality Transfer Using Sparteine as Chiral Ligand. *Chem. Commun.* **2014**, *50*, 14817.
(71) Kofron, W. G.; Baclawski, L. M. A Convenient Method for Estimation of Alkyllithium Concentrations. *J. Org. Chem.* **1976**, *41*, 1879.
(72) (a) Versteegen, R. M.; Rossin, R.; Hoeve, W. t.; Janssen, H. M.; Robillard, M. S. Click to Release: Instantaneous Doxorubicin Elimination upon Tetrazine Ligation. *Angew. Chem., Int. Ed.* **2013**, *52*, 14112. (b) Mack, D. J.; Guo, B.; Njardarson, J. T. Synthesis of Allylic and Homoallylic Alcohols from Unsaturated Cyclic Ethers Using a Mild and Selective C—O Reduction Approach. *Chem. Commun.* **2012**, *48*, 7844.

NOTE ADDED AFTER ASAP PUBLICATION

This paper was incorrectly published ASAP on August, 10 2021 due to a production error. The paper was corrected and the revised paper reposted on August 13, 2021.

https://doi.org/10.1021/jacs.1c06528
J. Am. Chem. Soc. 2021, 143, 13370—13381